

# Prediction of Inhibitory Activity of Epidermal Growth Factor Receptor Inhibitors Using Grid Search-Projection Pursuit Regression Method

Hongying Du<sup>1,2</sup>, Zhide Hu<sup>3</sup>, Andrea Bazzoli<sup>1</sup>, Yang Zhang<sup>1\*</sup>

**1** Center for Computational Medicine and Bioinformatics, University of Michigan, Ann Arbor, Michigan, United States of America, **2** Department of Public Health, Lanzhou University, Lanzhou, China, **3** Department of Chemistry, Lanzhou University, Lanzhou, China

## Abstract

The epidermal growth factor receptor (EGFR) protein tyrosine kinase (PTK) is an important protein target for anti-tumor drug discovery. To identify potential EGFR inhibitors, we conducted a quantitative structure–activity relationship (QSAR) study on the inhibitory activity of a series of quinazoline derivatives against EGFR tyrosine kinase. Two 2D-QSAR models were developed based on the best multi-linear regression (BMLR) and grid-search assisted projection pursuit regression (GS-PPR) methods. The results demonstrate that the inhibitory activity of quinazoline derivatives is strongly correlated with their polarizability, activation energy, mass distribution, connectivity, and branching information. Although the present investigation focused on EGFR, the approach provides a general avenue in the structure-based drug development of different protein receptor inhibitors.

**Citation:** Du H, Hu Z, Bazzoli A, Zhang Y (2011) Prediction of Inhibitory Activity of Epidermal Growth Factor Receptor Inhibitors Using Grid Search-Projection Pursuit Regression Method. PLoS ONE 6(7): e22367. doi:10.1371/journal.pone.0022367

**Editor:** Ying Xu, University of Georgia, United States of America

**Received:** January 31, 2011; **Accepted:** June 27, 2011; **Published:** July 21, 2011

**Copyright:** © 2011 Du et al. This is an open-access article distributed under the terms of the Creative Commons Attribution License, which permits unrestricted use, distribution, and reproduction in any medium, provided the original author and source are credited.

**Funding:** Funding was provided by the Alfred P. Sloan Foundation (<http://www.sloan.org/>), a NSF Career Award (DBI 1027394; <http://www.nsf.gov>), and the National Institute of General Medical Sciences (GM083107, GM084222; <http://www.nigms.nih.gov/>). The funders had no role in study design, data collection and analysis, decision to publish, or preparation of the manuscript.

**Competing Interests:** The authors have declared that no competing interests exist.

\* E-mail: zhng@umich.edu

## Introduction

The epidermal growth factor receptor (EGFR) is a transmembrane glycoprotein belonging to the human epidermal receptor (HER) family [1]. It is a type I tyrosine kinase receptor which plays a vital role in signal transduction pathways, regulating key cellular functions such as cell proliferation, survival, adhesion, migration, and differentiation [2–4]. The binding of a ligand to EGFR induces conformational changes within the receptor which increase its intrinsic catalytic activity of a tyrosine kinase and result in autophosphorylation, which is necessary for biological activity [5–7]. Mutations that lead to EGFR overexpression or overactivity have been associated with a variety of human tumors, including lung, bladder, colon, brain, and neck tumors [8–11]. Therefore, inhibitors of EGFR — inhibiting EGFR's kinase activity by competing with its cognate ligands — may potentially constitute a new class of effective drugs in clinical use or cancer therapy [12–14].

There are presently two main classes of EGFR inhibitors that can be used in cancer therapy. Both classes — the quinazoline derivatives [15–17] and the pyrimidin derivatives [18–20] — consist of ATP-competitive small molecules. To discover new effective EGFR inhibitors, investigators usually need to synthesize many compounds and test their corresponding activities by cell-based biological assay experiments, which is usually time-consuming and manpower expensive [21,22]. Consequently, it is of practical interest to develop reliable tools to predict biological activities before synthesis.

Quantitative structure–activity relationship (QSAR) is the most popular theoretical method for modeling a compound's biological

activity from its chemical structure [23–28]. Using this approach, scientists could predict the activities of series of newly designed drugs before making the final decision on whether or not to synthesize and assay them. The prediction is based on the structural descriptors of the molecular features that most account for the variations in biological activity. Furthermore, this method also can identify and describe the most important structural features of the compounds which are relevant to the variations in molecular properties, thus, it also gains an insight into the structural factors which affect the molecular properties. QSAR models of EGFR inhibitors have been recently investigated with encouraging results [29–33]. However, it is still vital to find faster and more reliable methods to assess the capability of EGFR inhibitors.

The exceedingly high dimension of the space of descriptors is a major problem in developing QSAR models. For this reason, increasing attention in the past several years has been devoted to QSAR models developed by projection pursuit regression (PPR) [34,35]. This is a general statistical technique that seeks the “interesting” projections of data from high-dimensional to lower-dimensional space, with the purpose of extracting the intrinsic structural information hidden in the high-dimensional data [36].

In the current investigation, two QSAR models were constructed from a set of known quinazoline-derivative EGFR inhibitors using multi-linear and non-linear regression approaches. The stability and accuracy of the regression models were assessed through an independent test set of EGFR inhibitors and a 5-fold cross validation approach. The study sheds light on the structure–activity relationship of this class of EGFR inhibitors and has the

potential prediction ability to identify new EGFR inhibitors. In addition, the explored structural features of the chemicals described here may facilitate the design of further new inhibitors with high  $pIC_{50}$  activities without any biological assay. Since the prediction relies exclusively on structural descriptors, the approach is expected to be of general use in drug design and discovery research.

## Materials and Methods

### Data set

The present investigation considered 128 quinazoline derivatives with known anti-cancer EGFR inhibitory activities [20,30,37–41]. The structures and activities of these compounds are listed in Table S1. The activities are expressed as  $pIC_{50}$  ( $= -\log(IC_{50})$ ) values, where  $IC_{50}$  (nM) represents the concentration of these compounds that produces 50% inhibition of the kinase activity of EGFR. Our aim was to exploit these known experimental activities to develop a QSAR model that would predict, based on selected chemo-physical molecular descriptors, the EGFR inhibitory activity of potential hits from the virtual screening of a compound library. To this purpose, the set of known EGFR inhibitors was randomly divided into two subsets: a training set of 103 compounds and a test set of 25 compounds (marked by asterisks in Table S1). The training set served to construct the QSAR models, while the test set was used for the model validation.

### Generation of the molecular descriptors

Two-dimensional structures of the compounds were drawn by using ISIS Draw 2.3 [42]. All the structures were fed into HyperChem 7.0 [43] and pre-optimized with the MM+ molecular-mechanics force field. The structures were then minimized in energy with the more precise semi-empirical AM1 method in MOPAC. After these steps, the DRAGON 5.4 [44] and CODESSA [45] programs were used to calculate the molecular descriptors from the structures, including 0D, 1D, 2D, and 3D descriptors from DRAGON [46], and constitutional, topological, geometrical, electrostatic, and quantum-chemical descriptors from CODESSA. 0D descriptors contain constitutional descriptors; 1D descriptors include functional-group counts and atom-centered fragments; 2D descriptors contain topological descriptors, connectivity indices, information indices, and eigenvalue-based indices; 3D descriptors represent some novel exclusive DRAGON descriptors and geometrical descriptors. There remained a total of 982 molecular descriptors after eliminating the constant and the highly-correlated descriptors. Then the generated descriptors were used to construct the regression models to predict the activities of the compounds. In order to clarify the whole procedure, its flowchart was drawn in Fig. 1.

### Best multi-linear regression

Best multi-linear regression (BMLR) refers to a multi-linear method which utilizes a more thorough procedure for finding the best linear regression model, based on a dependent variable and one or more independent variables [47]. The BMLR approach has several advantages, including high speed and no restriction on the size of the data set. It can either give a good estimation of the degree of correlation to expect from the data, or derive several best regression models. Moreover, it can highlight which descriptors have bad or missing values, which are insignificant, and which are highly inter-correlated. For these reasons, the BMLR method was chosen in this study to pre-select the most important descriptors and to construct the linear QSAR model.

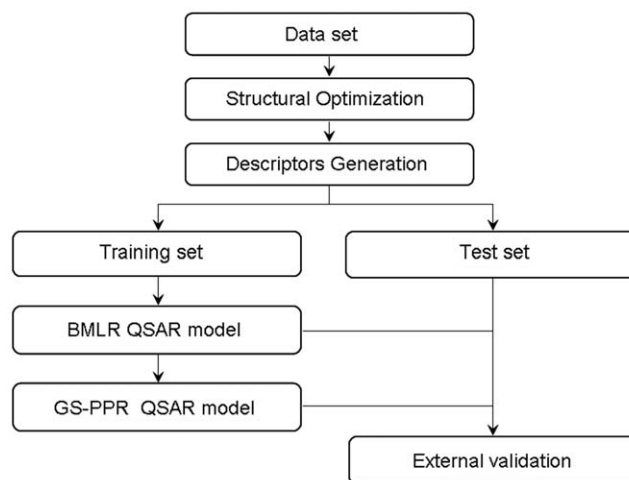


**Figure 1. Flowchart of the QSAR study.**  
doi:10.1371/journal.pone.0022367.g001

### Projection pursuit regression

Projection pursuit regression (PPR), developed by Friedman and Stuetzle [34], is a powerful method for seeking the interesting projections from high-dimensional spaces into lower-dimensional ones by means of linear projections. It can overcome the curse of dimensionality because it relies on estimation at most trivariate settings. At present, it has been successfully applied to tackle several chemical problems [36,48]. Friedman and Stuetzle's concept of PPR avoided many difficulties compared with other existing non-parametric regression procedures. Different from recursive partitioning regression, it does not split the predictor space into two regions, thereby allowing, when necessary, more complex models. In addition, interactions of predictor variables are directly considered because linear combinations of the predictors are modeled with general smooth functions. The basic theory of PPR can be found in references [34,35]. Here, only a brief description is given. Let  $X$  be a  $(k \times n)$  data matrix, where  $k$  is the number of observed variables and  $n$  is the number of units. Let also  $A$  be an  $m$ -dimensional orthonormal matrix  $A (m \times k)$ . Then the  $(m \times n)$  matrix  $Y = AX$  represents the coordinates of the projected data in the  $m$ -dimensional  $(m < k)$  space spanned by the rows of  $A$ . Because the number of possible projections is infinite, it is important to have a technique to pursue a finite sequence of projections that can reveal the most informative structures in the data. Projection pursuit (PP) is a tool that combines both ideas of projection and pursuit. [36] In a typical regression problem, PPR aims to approximate the regression pursuit function  $f(x)$  by a finite sum of ridge functions with suitable choices of  $\alpha_i$  and  $g_i$ .

$$f^{(p)}(x) = \sum_{i=1}^p g_i(\alpha_i^T x) \quad (1)$$

where the  $\alpha_i$  values are  $m \times n$  orthonormal matrices and  $p$  is the number of ridge functions. All programs implementing PPR were written in R-script under the R2.9.0 environment [49] and were executed on a Linux-operated Pentium IV with 4Gb of RAM.

### Evaluation of QSAR models

The predictive accuracy of the QSAR models was evaluated in terms of root-mean-square error (RMSE), defined as

$$RMSE = \sqrt{\frac{\sum_{i=1}^{n_s} (y_{ie} - y_{ip})^2}{n_s}} \quad (2)$$

where  $n_s$  is the number of known EGFR inhibitory compounds, and  $y_{ie}$  and  $y_{ip}$  are, respectively, the experimental and predicted EGFR inhibitory activities for the  $i_{th}$  compound.

## Results and Discussion

### Best multi-linear regression model

The best multi-linear regression (BMLR) method was utilized to develop a multi-linear QSAR model and select the most relevant molecular descriptors based on the training set. A variety set of descriptors have been tested for the selection of descriptors in different linear regression models. To avoid model “over-parameterization”, an increase of the squared Pearson correlation coefficient ( $R^2$ ) by less than 0.02 was chosen as the breakpoint criterion. Fig. 2 shows the number of descriptors *versus* the values of  $R^2$ , the leave-one-out (LOO) cross-validation ( $R_{CV}^2$ ), and Fisher’s  $F$ -test. It can be seen that nine descriptors are sufficient to optimize the regression model of the  $pIC_{50}$  of EGFR inhibitors. The optimum model is:

$$\left\{ \begin{array}{l} pIC_{50} = -183.56 + 4.501MEERCH - 143.52PMIC \\ \quad - 22.246(R4U+) + 2.569HATS3u + 11.265SIC1 \\ \quad - 3.621HATS5u - 1072.7ANR1C + 25.826LPI \quad (3) \\ \quad - 1.161EEig09d \\ N = 103, R^2 = 0.7835, R_{CV}^2 = 0.7335, S^2 = 0.3087, F = 37.39 \end{array} \right.$$

where  $N$  is the number of compounds in the training set,  $R^2$  is the squared Pearson correlation coefficient,  $R_{CV}^2$  is the squared cross-validation correlation coefficient,  $S^2$  is the squared standard deviation, and  $F$  is the Fisher  $F$ -test function. There are nine molecular descriptors selected. Three were calculated from CODESSA: *MEERCH* (Min e-e repulsion for a C-H bond),

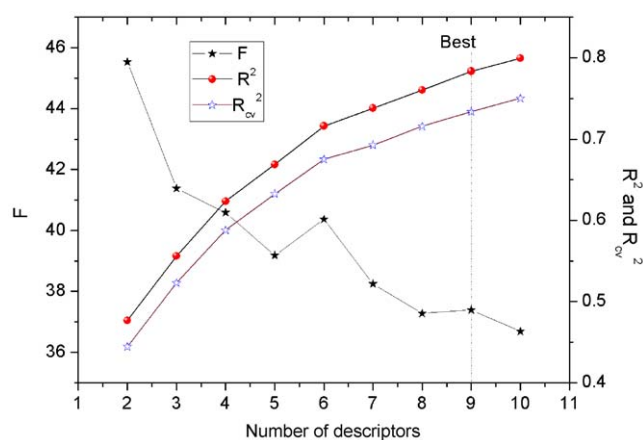


**Figure 2. Influence of the number of descriptors on the square of Pearson correlation coefficient ( $R^2$ ), leave one out (LOO) cross-validation coefficient ( $R_{CV}^2$ ), and  $F$ -values of the BMLR models.**

doi:10.1371/journal.pone.0022367.g002

*PMIC* (Principal moment of inertia C), and *ANR1C* (Avg nucleoph. react. index for a C atom); the other five descriptors were obtained from DRAGON: *R4U+*, *HATS3u*, *SIC1*, *HATS5u*, *LPI*, and *EEig09d*.

The descriptor *MEERCH* is a quantum mechanical energy-related descriptor, used to characterize the total energy of the molecule at different energy scales and intramolecular energy distribution using different partitioning schemes. It is calculated as follows:

$$E_{ee(CH)} = \sum_{\mu, \nu \in C} \sum_{\lambda, \sigma \in H} P_{\mu\nu} P_{\lambda\sigma} \langle \mu\nu | \lambda\sigma \rangle \quad (4)$$

where  $P_{\mu\nu}$  and  $P_{\lambda\sigma}$  are the density matrix elements and  $\langle \mu\nu | \lambda\sigma \rangle$  are the electron repulsion integrals on the atomic basis  $\{\mu\nu | \lambda\sigma\}$ . This descriptor refers to the electron repulsion-driven process in the molecule and can be related to the conformational (rotational, inversional) changes or atomic reactivity in the molecule [50]. The descriptor *PMIC* is a geometrical descriptor which related with their 3D-coordinates information of the atoms in the molecule. It is equal to  $\sum_i m_i r_{iz}^2$ , where  $m_i$  is the mass of the  $i$ th atom and  $r_{iz}$

denotes the distance of the  $i$ th atomic nucleus from the main rotational  $z$ -axis of the molecule [51]. As an expression of the principal moment of inertia, this descriptor characterizes the distribution of mass in the molecule. The descriptor *ANR1C* is a quantum chemical descriptor of the average value of the atom C nucleophilic ( $N_A$ ) Fukui reactivity indices [52] for carbon in the molecule, which are defined as follows:

$$N_A = \sum_{i \in A} C_{iHOMO}^2 / (1 - \varepsilon_{HOMO}) \quad (5)$$

where,  $C_{iHOMO}$  denotes the  $i$ th AO coefficient for the highest occupied molecular orbital (HOMO), and  $\varepsilon_{HOMO}$  is the energy of these orbitals. The reactivity indices estimate the relative reactivity of carbon in the molecule for the given series of compounds and are related to the activation energy of the corresponding chemical reaction. The descriptor *R4U+*, which belongs to the GETAWAY (GEometry, Topology and Atom-Weights Assembly) descriptors, is the R maximal autocorrelation coefficient of lag 4/unweighted and R autocorrelation coefficient of lag 5/unweighted, respectively. The  $R$  and  $R+$  descriptors are analogously obtained from the leverage/geometry matrix [53]. The descriptors *HATS3u* and *HATS5u* are GETAWAY descriptors defined by the leverage-weighted autocorrelation of lag 3 and lag 5/unweighted, respectively. They take into account 3D molecular geometry by using the leverage values as atom weights [53]. The descriptor *SIC1* is one of the information indices of the molecule, the name standing for Structural Information Content index (neighborhood symmetry of 1-order). It is defined by the application of information theory to the chemical and bonding neighborhood of the atoms in the molecule [54]; thus it might reflect molecular polarity and polarizability. *LPI* is the Lovasz–Pelikan index or leading eigen value, and is a topological descriptor. It has been suggested as an index of molecular branching, the smallest values corresponding to chin graphs and the highest to the most branched graphs. In equation (3) the *LPI* contribution has a positive sign, which indicates that the  $IC_{50}$  is inversely related to this descriptor; therefore, increasing the branching of molecules leads to a decrease in their  $IC_{50}$ . The last descriptor, *EEig09d*, is a topological molecular descriptor. It is defined as Eigenvalue 09 from the edge adj. matrix weighted by dipole moments, and encodes the connectivity between graph edges.

From the above presentation, it is concluded that the selected descriptors can be interpreted reasonably, and the inhibition ability of quinazoline derivatives mainly depends on the following properties: polarizability, activation energy, mass distribution, connectivity, and branching information. In order to facilitate our understanding of the main features of EGFR inhibitors, we also investigated one of the existing X-ray crystal structures of ligand-bound EGFR [55]. As shown in Fig. 3, an amide nitrogen donor of the ligand together with the carboxyl group of MET769 form a hydrogen bond in the EGFR hinge region. Hydrogen-bond interactions play a crucial role in ligand-protein binding; however polarizability was one of the critical factors in forming the interaction in a broader sense, involving both the hydrophilic and hydrophobic regions of the receptor. In fact, the polarizability of the ligand is essential to stabilize any generated hydrogen bonds. Consistently with our QSAR study, Vema et al. [30], who docked the selected drugs to the active binding site of the same EGFR kinase domain, found that the regions of the receptor surface around different branching places exhibited different electronic properties, either electronegative or electropositive. Thus the connectivity and branching information contributed greatly to the docking and interaction of the ligands with EGFR. Such information was helpful to clarify the mechanisms of molecular docking encountered in drug-discovery studies.

The correlation matrix of these selected descriptors is shown by a heat map in Fig. 4, produced with the *R*-package *gplots* [57]. The linear correlation coefficients of all descriptor pairs are at most equal to 0.80 and the majority of them are below 0.3, which demonstrates the relative independence of the selected descriptors. Furthermore, the hierarchical clustering reveals noteworthy contributions of the nature of the different selected molecular descriptors. For example, descriptors *EEig09d* and *LPI*, accounting primarily for the connectivity and branching information of the molecule, cluster together. Similarly, descriptors *HATS3u*, *HATS5u*

and *R4u* belong to GETEWAY descriptors, and they are in the same cluster, by representing the information of different atoms in the molecules, and all related with the Cartesian coordinates of the molecule atoms (including hydrogen) in a chosen conformation [58]. Finally, the six descriptors which were calculated from DRAGON were clustered together; and they can be viewed as describing the intrinsic property of the molecules. Descriptors ANRIC and MEERCH are clustered together. They were calculated from quantum chemistry methods, and represent their electron and nucleoph properties in the molecules. They related with the activation energy and electronegativity of the molecule, respectively, and simulated the interactions with other molecules.

The predicted  $pIC_{50}$  activity values for all the known EGFR inhibitors, including the training and test sets are given in Table S1, where the experimental  $pIC_{50}$  values are also listed. Fig. 5 shows the predicted *versus* the experimental  $pIC_{50}$  values for the training and test sets, respectively. There is an obvious correlation between the predicted and experimental values of  $pIC_{50}$ , with the square of Pearson correlation coefficients 0.7835 and 0.7595 for the training and test sets, respectively. The whole statistical parameters of the BMLR model are given in Table 1. There is no notable difference in the correlation coefficient for the test and training data, confirming that the model was indeed not “over-trained”.

### Principal component analysis of the selected descriptors

Principal component analysis (PCA) is always used to reduce the dimensionality of multidimensional variables and analyze complex intrinsic features among variables. In the current research, PCA method was performed using the selected nine descriptors with the aim to show the spatial location of every drug, and also check the distribution of the drugs in the training and test sets. The two major principal components were given here. The explained variance of these two components is 50.38% of the total

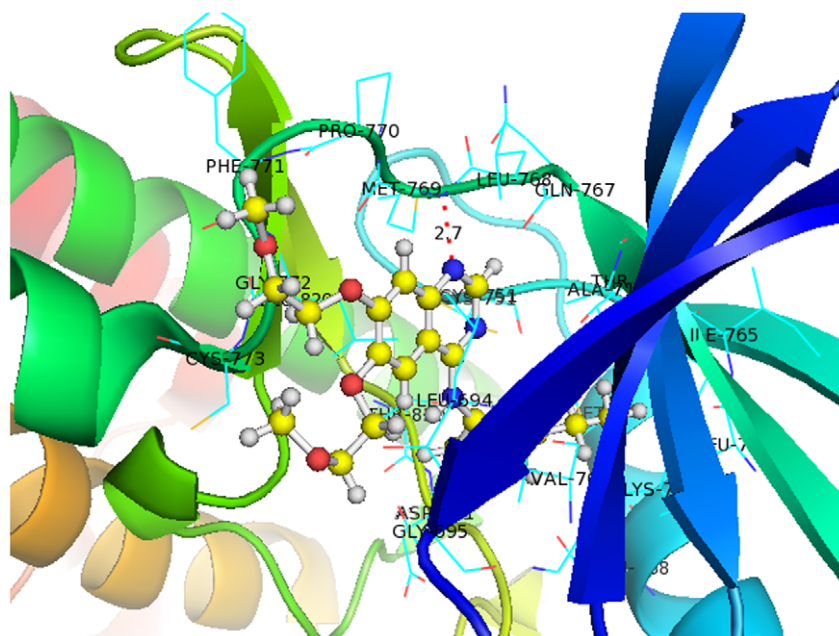


**Figure 3. Crystal structure of EGFR bound to the 4-anilinoquinazoline inhibitor Erlotinib (PDB ID: 1M17).** EGFR is represented by a cartoon model, with the side chains of the binding site wire-framed in cyan and labeled. The inhibitor is represented by a stick-and-ball model, where carbons are colored in yellow, nitrogens in blue, oxygens in red, and hydrogens in light grey. The hydrogen bond between an amide nitrogen donor of the ligand and the carboxyl group of MET769 in the receptor is plotted as a red dotted line. Figure produced with the PyMOL program [56]. doi:10.1371/journal.pone.0022367.g003

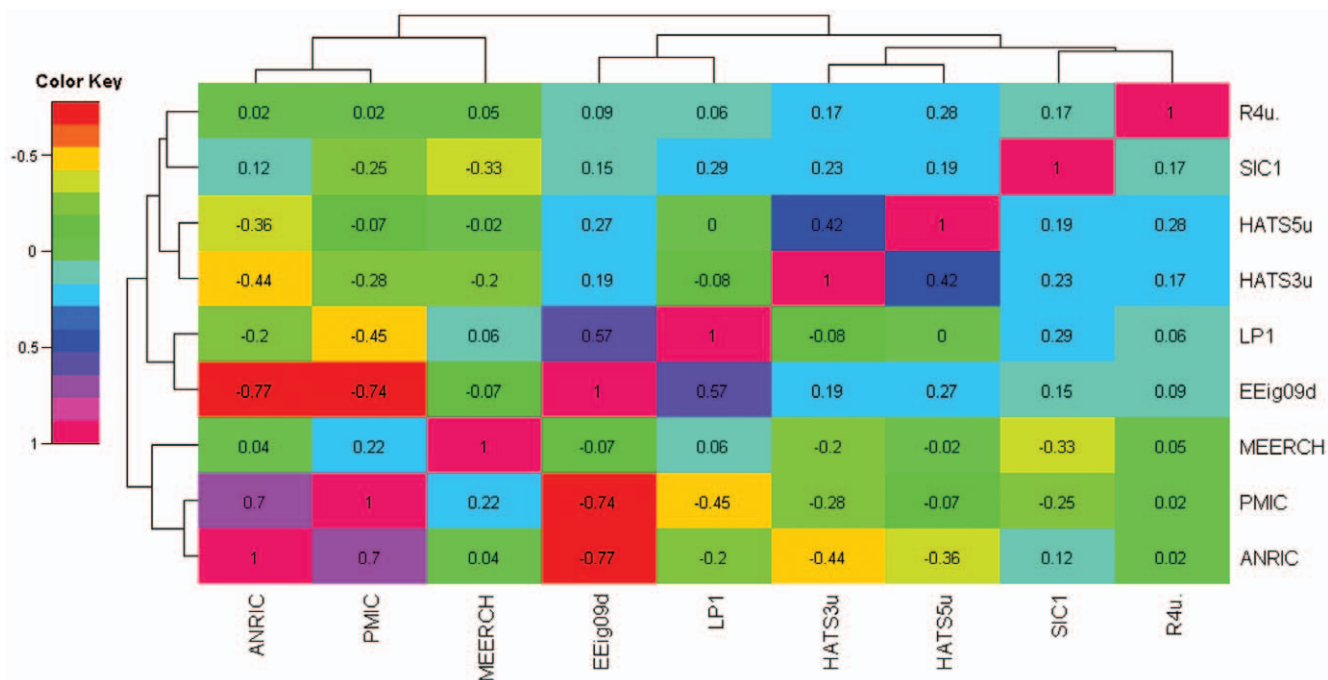


**Figure 4. Heat maps of the correlation matrix of the molecular descriptors.** Rows and columns are ordered according to a hierarchical clustering (cluster tree lines on the side and top) of the selected molecular descriptors codes.  
doi:10.1371/journal.pone.0022367.g004

information (PC1 explained variance equals to 33.98%), thus the most useful information was interpreted in the first two PCs. Fig. 6 illustrates a loading plot of these two components for the training and test sets. From this figure, it can be seen that the samples in the both training and test sets are well balanced and evenly scattered over the whole space occupied by dissimilar plotting symbols. This confirmed that the drugs in the training set can be used as the representative samples of the whole data set, and the splitting method is also reliable for the assessment of the predictive ability and performance of different models.

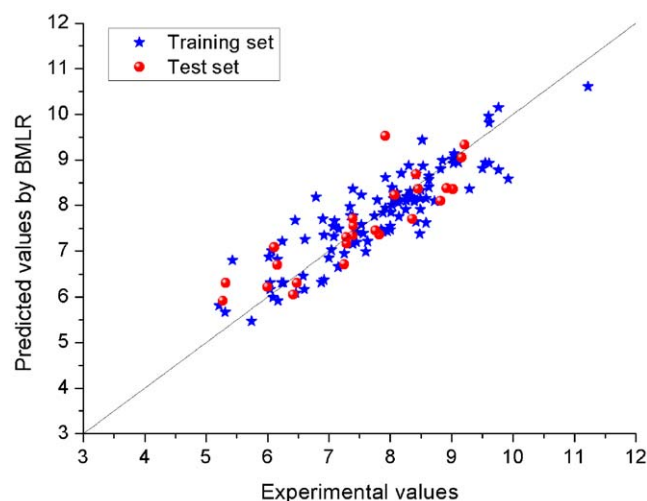


**Figure 5. Plot for the training and test EGFR inhibitors of the  $pIC_{50}$  values predicted by the BMLR method versus the experimental  $pIC_{50}$  values.**  
doi:10.1371/journal.pone.0022367.g005

Furthermore, it also illustrates that the nine selected variables have various directions and various sizes in this figure. These descriptors clearly distributed in the four different regions of rectangular coordinate system: R4u+, HATS3u, HATS5u and SIC1 in quadrant (I); RMIC and ANRIC in quadrant (II), MEERCH in quadrant (III), and EEig09d and LP1 in the last quadrant (IV). All these information explored here consisted with the results of former cluster analysis.

#### Projection pursuit regression model

After building the linear BMLR model, projection pursuit regression (PPR) was applied to effectively project the nine descriptors to a lower-dimensional space, and to perform a non-linear regression in this lower dimensional space; the goal of the regression was to correlate the EGFR inhibitory activity with the structural information. The PPR approach requires the optimiza-

**Table 1.** Comparison of the statistical results between the BMLR and GS-PPR models.

| Parameter | Sets         | BMLR   | GS-PPR | Ref. [30] |
|-----------|--------------|--------|--------|-----------|
| $R^2$     | Training set | 0.7835 | 0.8534 | 0.8492    |
|           | Test set     | 0.7595 | 0.8116 | 0.5325    |
|           | All set      | 0.7808 | 0.8461 | 0.7691    |
| RMSE      | Training set | 0.5656 | 0.4345 | 0.4347    |
|           | Test set     | 0.5280 | 0.5040 | 0.8455    |
|           | All set      | 0.5355 | 0.4489 | 0.5514    |

**Note:** BMLR: best multi-linear regression; GS-PPR: grid search-projection pursuit regression.  $R^2$ : squared Pearson correlation coefficient between the experimental and predicted  $pIC_{50}$  values. RMSE: root-mean-square error between the experimental and predicted  $pIC_{50}$  values.  
doi:10.1371/journal.pone.0022367.t001

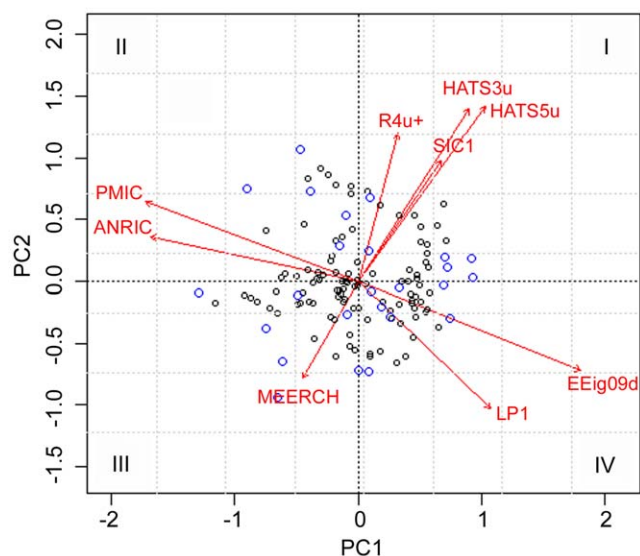


**Figure 6. Principal component analysis of the nine selected descriptors.** Arrows indicate the directions of the variable vectors in the principal component space. Black circles denote compounds from the training set, blue circles those from the test set.  
doi:10.1371/journal.pone.0022367.g006

tion of several parameters, including ‘nterms’ and ‘max.terms’, which represent the number of ridge terms included in the final model and the maximum number of ridge terms for building the model, respectively; the parameter ‘df’ defines the smoothness of each ridge term by the requested equivalent degrees of freedom; the levels of optimization (parameter ‘optlevel’) differ in how thoroughly the models are refitted. At level 0 the existing ridge terms are not refitted. At level 1 the projection directions are not refitted, but the ridge functions and the regression coefficients are. Levels 2 and 3 refit all of the terms and are equivalent for one response; level 3 is more careful to re-balance the contributions from each regression at each step and so is slightly less likely to converge to a saddle point of the sum of squares criterion. Since the traditional PPR method usually adopts a single-factor correction

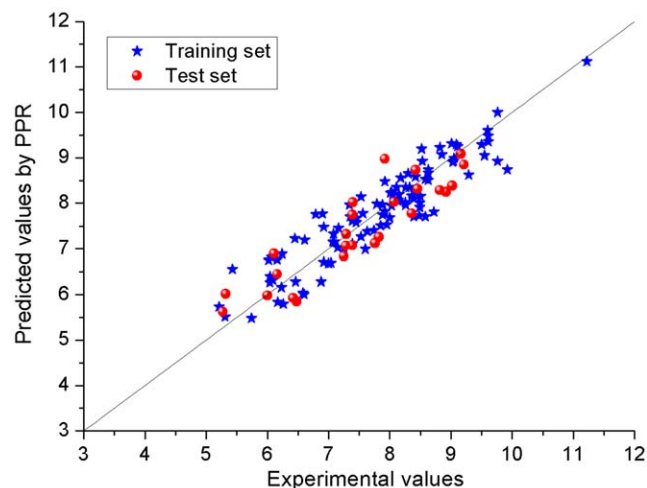


**Figure 8. Plot for the training and test EGFR inhibitors of the  $pIC_{50}$  values predicted by the GS-PPR method versus the experimental  $pIC_{50}$  values.**  
doi:10.1371/journal.pone.0022367.g008

analysis, the models they produce tend to be only local optima. Here, the grid-search (GS) method was employed, which relies instead on multi-factor correction analysis, thereby producing a final model that is generally closer to the global optimum [59]. The results indicate that the ‘optlevel’ and ‘df’ parameters influenced the optimization only slightly. Figures 7(a) and 7(b) show the values of  $R^2$  and  $RMSE$ , respectively, as a function of ‘max.terms’ and ‘nterms’, the two most important optimization parameters. The optimum values of ‘nterms’, ‘max.terms’, ‘df’, and ‘optlevel’ are determined as 3, 7, 8, and 1, respectively. In order to assess the internal predictability of the training set, a 5-fold cross validation is typically used, providing an estimate for the mean performance of a model. The values of the statistical parameters of the 5-fold cross validation were  $R_{cv}^2 = 0.7709$ , and  $RMSE = 0.6186$ . Furthermore, the results of the test set prediction were confirmed by the external prediction of the regression model. These data suggest that the model we proposed has a robust prediction power.

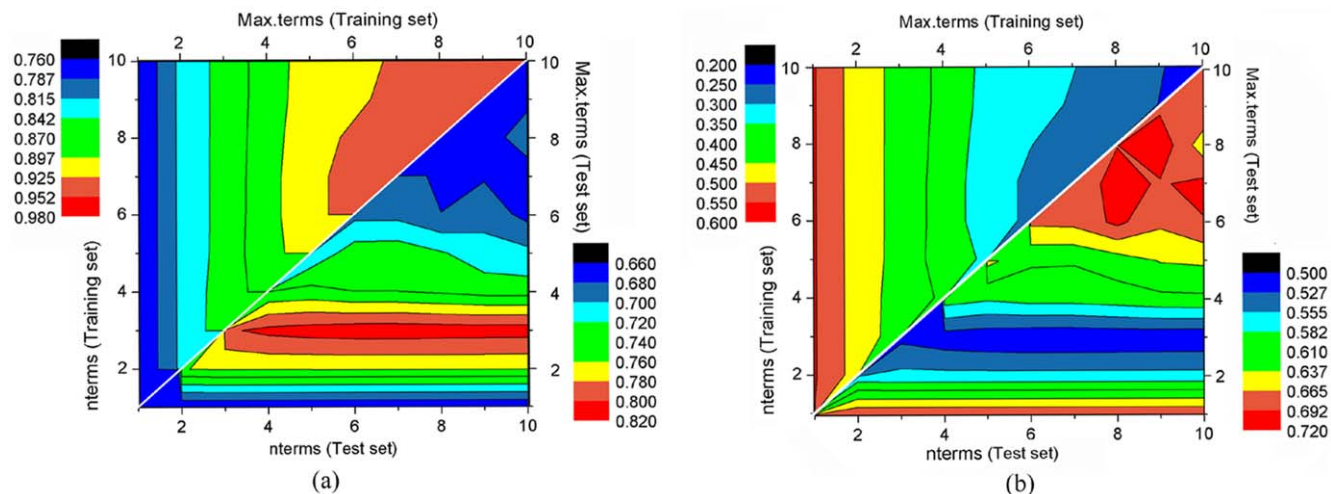


**Figure 7. Statistical parameters of the training set and the test set during the optimization process of the PPR parameters by the grid search method.** (a):  $R^2$ , (b):  $RMSE$ .  
doi:10.1371/journal.pone.0022367.g007

The predicted results and the statistical parameters of the optimal PPR model are shown in Tables S1 and 1, respectively. The scatter plot of the predicted *versus* the experimental  $pIC_{50}$  values is given in Fig. 8. From Fig. 8 and Table S1 it can be seen that the predicted values are in good agreement with the experimental values for almost all the compounds.

### Comparison of results of obtained by different models

In order to check the superiority of these two different models (BMLR and GS-PPR), the predicted results and the statistical parameters for the training and the test sets were collected together and shown in Tables S1 and 1, separately. As it can be seen from this table, the improved non-linear regression method GS-PPR outperforms the BMLR model according to the  $R^2$  and  $RMSE$ , and it shows much better predictive ability, and its corresponding predicted results indicate an appropriate fit of the model. Previously, Vema et al. [30] used the 3D-QSAR method molecular field analysis (MFA) and receptor surface analysis (RSA) to investigate the inhibitory activities of the same data set. The squared Pearson correlation coefficient ( $R^2$ ) of their best model (RSA) is 0.8492 for the training set and 0.5325 for the test set. All of the other statistical parameters were collected in Table 1. By comparing these results, it can be concluded that the GS-PPR method is a simple but with powerful predictive capability tool as to the inhibitory activity of potential anti-EGFR drugs.

### Conclusions

We have explored the features of potential inhibitors of epidermal growth factor receptor, a vital protein target involved in clinical anticancer therapies, based on linear and non-linear QSAR models. A new non-linear QSAR method for the

prediction of EGFR inhibitory activity was developed, which combines the grid search (GS) and projection pursuit regression (PPR) techniques to infer biological activity from a set of molecular descriptors; these were selected by the best multi-linear regression (BMLR) exclusively from structural information. The GS-PPR model showed a better predictive ability than the traditional linear QSAR model, demonstrating that the combination of PPR and GS is a valuable strategy for QSAR model building, at least for the prediction of EGFR inhibitors. In addition, this investigation shows that the structural features of quinazoline derivatives are most relevant to quinazoline derivatives inhibition — namely, polarizability, activation energy, mass distribution, connectivity, and branching. The set of EGFR inhibitors, real or hypothetical, which can possibly be examined by such studies, is large and heterogeneous, due to the purely structural nature of the molecular descriptors. The approach can be easily extended to other cheminformatic and bioinformatics investigations, since the small number of parameters to be optimized makes the training procedure generally simple.

### Supporting Information

**Table S1** Structures and EGFR inhibitory activities of 128 known EGFR inhibitors. (PDF)

### Author Contributions

Conceived and designed the experiments: HYD YZ. Performed the experiments: HYD. Analyzed the data: HYD ZDH AB YZ. Contributed reagents/materials/analysis tools: HYD ZDH YZ. Wrote the paper: HYD AB YZ.

### References

- Ullrich A, Schlessinger J (1990) Signal transduction by receptors with tyrosine kinase activity. *Cell* 61: 203–212.
- Verbeek BS, Adriaansen-Slot SS, Vroom TM, Beckers T, Rijkse G (1998) Overexpression of EGFR and c-erbB2 causes enhanced cell migration in human breast cancer cells and NIH3T3 fibroblasts. *FEBS Letters* 425: 145–150.
- Wells A (1999) EGF receptor. *International Journal of Biochemistry & Cell Biology* 31: 637–643.
- Yarden Y, Sliwkowski MX (2001) Untangling the ErbB signalling network. *Nature Reviews Molecular Cell Biology* 2: 127–137.
- Hsuan JJ (1993) Oncogene regulation by growth-factors. *Anticancer Research* 13: 2521–2532.
- Soler C, Beguinot L, Carpenter G (1994) Individual epidermal growth-factor receptor autophosphorylation sites do not stringently define association motifs for several SH2-containing proteins. *Journal of Biological Chemistry* 269: 12320–12324.
- Voldborg BR, Damstrup L, Spang-Thomsen M, Poulsen HS (1997) Epidermal growth factor receptor (EGFR) and EGFR mutations, function and possible role in clinical trials. *Annals of Oncology* 8: 1197–1206.
- Toyoshima E, Ohsaki Y, Nishigaki Y, Fujimoto Y, Kohgo Y, et al. (2001) Expression of syndecan-1 is common in human lung cancers independent of expression of epidermal growth factor receptor. *Lung Cancer* 31: 193–202.
- Gross ME, Zorbas MA, Danels YJ, Garcia R, Gallick GE, et al. (1991) Cellular growth-response to epidermal growth-factor in colon-carcinoma cells with an amplified epidermal growth-factor receptor derived from a familial adenomatous polyposis patient. *Cancer Research* 51: 1452–1459.
- Damstrup L, Rygaard K, Spangthomsen M, Poulsen HS (1992) Expression of the epidermal growth-factor receptor in human small-cell lung-cancer cell-lines. *Cancer Research* 52: 3089–3093.
- van der Veecken J, Oliveira S, Schifferers RM, Storm G, Henegouwen P, et al. (2009) Crosstalk between epidermal growth factor receptor- and insulin-like growth factor-1 receptor signaling: implications for cancer therapy. *Current Cancer Drug Targets* 9: 748–760.
- Bridges AJ (1999) The rationale and strategy used to develop a series of highly potent, irreversible, inhibitors of the epidermal growth factor receptor family of tyrosine kinases. *Current Medicinal Chemistry* 6: 825–843.
- Boschelli DH (1999) Small molecule inhibitors of receptor tyrosine kinases. *Drugs of the Future* 24: 515–537.
- Ma XH, Wang R, Tan CY, Jiang YY, Lu T, et al. (2010) Virtual screening of selective multitarget kinase inhibitors by combinatorial support vector machines. *Molecular Pharmaceutics* 7: 1545–1560.
- Abouzid K, Shouman S (2008) Design, synthesis and in vitro antitumor activity of 4-aminoquinoline and 4-aminoquinazoline derivatives targeting EGFR tyrosine kinase. *Biorganic & Medicinal Chemistry* 16: 7543–7551.
- Wissner A, Overbeek E, Reich MF, Floyd MB, Johnson BD, et al. (2003) Synthesis and structure-activity relationships of 6,7-disubstituted 4-anilinoquinoline-3-carbonitriles. The design of an orally active, irreversible inhibitor of the tyrosine kinase activity of the epidermal growth factor receptor (EGFR) and the human epidermal growth factor receptor-2 (HER-2). *Journal of Medicinal Chemistry* 46: 49–63.
- Pawar VG, Sos ML, Rode HB, Rabiller M, Heyneck S, et al. (2010) Synthesis and biological evaluation of 4-anilinoquinolines as potent inhibitors of epidermal growth factor receptor. *Journal of Medicinal Chemistry* 53: 2892–2901.
- Klutchko SR, Hamby JM, Boschelli DH, Wu ZP, Kraker AJ, et al. (1998) 2-substituted aminopyrido 2,3-d pyrimidin-7(8H) ones. Structure-activity relationships against selected tyrosine kinases and in vitro and in vivo anticancer activity. *Journal of Medicinal Chemistry* 41: 3276–3292.
- Solca FF, Baum A, Langkopf E, Dahmann G, Heider KH, et al. (2004) Inhibition of epidermal growth factor receptor activity by two pyrimidopyrimidine derivatives. *Journal of Pharmacology and Experimental Therapeutics* 311: 502–509.
- Thompson AM, Bridges AJ, Fry DW, Kraker AJ, Denny WA (1995) Tyrosine kinase inhibitors. 7. 7-amino-4-(phenylamino)pyrido 4,3-d pyrimidines and 7-amino-4-(phenylmethyl)amino pyrido 4,3-d pyrimidines - a new class of inhibitors of the tyrosine kinase-activity of the epidermal growth-factor receptor. *Journal of Medicinal Chemistry* 38: 3780–3788.
- Ding K, Lu YP, Nikolovska-Coleska Z, Wang GP, Qiu S, et al. (2006) Structure-based design of spiro-oxindoles as potent, specific small-molecule inhibitors of the MDM2-p53 interaction. *Journal of Medicinal Chemistry* 49: 3432–3435.
- Li N, Thompson S, Schultz DC, Zhu WL, Jiang HL, et al. (2010) Discovery of selective inhibitors against EBNA1 via high throughput in silico virtual screening. *Plos One* 5: e10126–e10129.
- Nunez MB, Maguna FP, Okulik NB, Castro EA (2004) QSAR modeling of the MAO inhibitory activity of xanthenes derivatives. *Biorganic & Medicinal Chemistry Letters* 14: 5611–5617.
- Hansch C, Verma RP (2009) Overcoming tumor drug resistance with C2-modified 10-deacetyl-7-propionyl cephalomannines: A QSAR study. *Molecular Pharmaceutics* 6: 849–860.
- Mandal AS, Roy K (2009) Predictive QSAR modeling of HIV reverse transcriptase inhibitor TIBO derivatives. *European Journal of Medicinal Chemistry* 44: 1509–1524.

26. Liu FP, Liang YZ, Cao CZ (2006) QSPR modeling of thermal conductivity detection response factors for diverse organic compound. *Chemometrics and Intelligent Laboratory Systems* 81: 120–126.
27. Liu HX, Gramatica P (2007) QSAR study of selective ligands for the thyroid hormone receptor beta. *Bioorganic & Medicinal Chemistry* 15: 5251–5261.
28. Verma RP, Hansch C (2010) QSAR modeling of taxane analogues against colon cancer. *Eur J Med Chem* 45: 1470–1477.
29. Pasha FA, Muddassar M, Srivastava AK, Cho SJ (2010) In silico QSAR studies of anilinoquinolines as EGFR inhibitors. *Journal of Molecular Modeling* 16: 263–277.
30. Vema A, Panigrahi SK, Rambabu G, Gopalakrishnan B, Sarma J, et al. (2003) Design of EGFR kinase inhibitors: A ligand-based approach and its confirmation with structure-based studies. *Bioorganic & Medicinal Chemistry* 11: 4643–4653.
31. Szántai-Kis C, Kóvesdi I, Eros D, Bánhegyi P, Ullrich A, et al. (2006) Prediction oriented QSAR modelling of EGFR inhibition. *Current Medicinal Chemistry* 13: 277–287.
32. La Motta C, Sartini S, Tuccinardi T, Nerini E, Da Settimo F, et al. (2009) Computational studies of epidermal growth factor receptor: Docking reliability, three-dimensional quantitative structure-activity relationship analysis, and virtual screening studies. *Journal of Medicinal Chemistry* 52: 964–975.
33. Shi WM, Shen Q, Kong W, Ye BX (2007) QSAR analysis of tyrosine kinase inhibitor using modified ant colony optimization and multiple linear regression. *European Journal of Medicinal Chemistry* 42: 81–86.
34. Friedman JH, Stuetzle W (1981) Projection pursuit regression. *Journal of the American Statistical Association* 76: 817–823.
35. Huber PJ (1985) Projection pursuit. *Annals of Statistics* 13: 435–475.
36. Donoho D, Johnstone I, Rousseeuw P, Stahel W (1985) Projection pursuit - Discussion. *Annals of Statistics* 13: 496–500.
37. Rewcastle GW, Denny WA, Bridges AJ, Zhou HR, Cody DR, et al. (1995) Tyrosine kinase inhibitors .5. synthesis and structure - activity - relationships for 4-(phenylmethylamino)-quinazolines and 4-(phenylamino)quinazolines as potent adenosine 5'-triphosphate binding-site inhibitors of the tyrosine kinase domain of the epidermal growth-factor receptor. *Journal of Medicinal Chemistry* 38: 3482–3487.
38. Bridges AJ, Zhou H, Cody DR, Rewcastle GW, McMichael A, et al. (1996) Tyrosine kinase inhibitors .8. An unusually steep structure-activity relationship for analogues of 4-(3-bromoanilino)-6,7-dimethoxyquinazoline (PD 153035), a potent inhibitor of the epidermal growth factor receptor. *Journal of Medicinal Chemistry* 39: 267–276.
39. Rewcastle GW, Palmer BD, Thompson AM, Bridges AJ, Cody DR, et al. (1996) Tyrosine kinase inhibitors .10. Isomeric 4-(3-bromophenylamino)pyrido d-pyrimidines are potent ATP-binding site inhibitors of the tyrosine kinase function of the epidermal growth factor receptor. *Journal of Medicinal Chemistry* 39: 1823–1835.
40. Rewcastle GW, Bridges AJ, Fry DW, Rubin JR, Denny WA (1997) Tyrosine kinase inhibitors .12. Synthesis and structure-activity relationships for 6-substituted 4-(phenylamino)pyrimido 5,4-d pyrimidines designed as inhibitors of the epidermal growth factor receptor. *Journal of Medicinal Chemistry* 40: 1820–1826.
41. Thompson AM, Murray DK, Elliott WL, Fry DW, Nelson JA, et al. (1997) Tyrosine kinase inhibitors .13. Structure-activity relationships for soluble 7-substituted 4-(3-bromophenylamino)pyrido 4,3-d pyrimidines designed as inhibitors of the tyrosine kinase activity of the epidermal growth factor receptor. *Journal of Medicinal Chemistry* 40: 3915–3925.
42. ISIS Draw2. 3 (1990–2000) MDLInformation Systems, Inc.
43. HyperChem, Release 6.0 for Windows, Hypercube, Inc., 2000.
44. Todeschini R, Consonni V, Mauri A, Pavan M (2006) DRAGONs Software for the calculation of molecular descriptors, version 5.4 for Windows. Milan, Italy: Talete srl.
45. Katritzky AR, Lobanov VS, Karelson M (1995) CODESSA Version 2.0 Reference Manual Gainesville Florida: University of Florida.
46. Todeschini R, Consonni V (2000) Handbook of Molecular Descriptors; Wiley-VCH. Weinheim, Germany.
47. Katritzky AR, Lobanov VS, Karelson M (1995) CODESSA: Training Manual. Gainesville, Florida: University of Florida.
48. Du HY, Wang J, Hu ZD, Yao XJ, Zhang XY (2008) Prediction of fungicidal activities of rice blast disease based on least-squares support vector machines and project pursuit regression. *Journal of Agricultural and Food Chemistry* 56: 10785–10792.
49. Birattari M, Bontempi G (2003) R manuals, The R Development Core Team.
50. Strouf O (1986) Chemical Pattern Recognition New York: Wiley.
51. Weast RC (1974) Handbook of Chemistry and Physics. Cleveland OH: CRC Press. pp F-112.
52. Fukui K (1975) Theory of Orientation and Stereoselection Berlin: Springer-Verlag.
53. Consonni V, Todeschini R, Pavan M (2002) Structure/response correlations and similarity/diversity analysis by GETAWAY descriptors. 1. Theory of the novel 3D molecular descriptors. *Journal of Chemical Information and Computer Sciences* 42: 682–692.
54. Basak SC, Mills D, Hawkins DM (2008) Predicting allergic contact dermatitis: a hierarchical structure-activity relationship (SAR) approach to chemical classification using topological and quantum chemical descriptors. *Journal of Computer-Aided Molecular Design* 22: 339–343.
55. Stamos J, Sliwkowski MX, Eigenbrot C (2002) Structure of the epidermal growth factor receptor kinase domain alone and in complex with a 4-anilinoquinazoline inhibitor. *Journal of Biological Chemistry* 277: 46265–46272.
56. Delano WL (2002) The PyMol Molecular Graphics System Delano Scientific. San Carlos, CA, USA: DeLano Scientific.
57. The R Project for Statistical Computing. <http://www.r-project.org/> (Accessed May 21, 2010).
58. Puzyn T, Leszczynski J, Cronin MT (2010) Recent Advances in QSAR Studies Methods and Applications: Springer Dordrecht Heidelberg London New York.
59. Du HY, Wang J, Zhang XY, Hu ZD (2008) A novel quantitative structure-activity relationship method to predict the affinities of MT3 melatonin binding site. *European Journal of Medicinal Chemistry* 43: 2861–2869.